59. Variable-Temperature and Variable-Pressure ^{17}O-NMR Study of Water Exchange of Hexaaquaaluminium(III)[1][2]

by **Deirdre Hugi-Cleary, Lothar Helm,** and **André E. Merbach***

Institut de chimie minérale et analytique de l'Université de Lausanne, Place du Château 3, CH-1005 Lausanne

(11.I.85)

The transverse relaxation rate of H_2O in $Al(H_2O)_6^{3+}$ has been measured as a function of temperature (255 to 417 K) and pressure (up to 220 MPa) using the ^{17}O-NMR line-broadening technique, in the presence of Mn(II) as a relaxation agent. At high temperatures the relaxation rate is governed by chemical exchange with bulk H_2O, whereas at low temperatures quadrupolar relaxation is prevailing. Low-temperature fast-injection ^{17}O-NMR was used to extend the accessible kinetic domain. The samples studied contained Al^{3+} (0.5 *m*), Mn^{2+} (0.2–0.5 *m*), H^+ (0.2–3.1 *m*) and ^{17}O-enriched (20–40%) H_2O. Non-coordinating perchlorate was used as counter ion. The following H_2O exchange parameters were obtained: $k_{ex}^{298} = (1.29 \pm 0.04)\ s^{-1}$, $\Delta H^* = (84.7 \pm 0.3)\ kJ\ mol^{-1}$, $\Delta S^* = +(41.6 \pm 0.9)\ J\ K^{-1}\ mol^{-1}$, and $\Delta V^*_{ex} = +(5.7 \pm 0.2)\ cm^3\ mol^{-1}$, indicating a dissociative interchange, I_d, mechanism. These results of H_2O exchange on $Al(H_2O)_6^{3+}$ are discussed together with the available complex-formation rate data and permit also the assignment of I_d mechanisms to these latter reactions.

Introduction. – The volume of activation, ΔV^*, has proven to be a unique kinetic parameter for mechanistic assignment of H_2O-exchange reactions on metal ions. In particular, the change in ΔV^* from negative to positive values across the series for the divalent first-row transition-metal ions was the first indication of a mechanistic changeover along this series. The available ΔV^*'s for H_2O exchange on hexaaqua trivalent metal ions are all negative, indicative of association interchange mechanisms: −8.9 cm^3mol^{-1} for V^{3+} [1], −9.6 cm^3mol^{-1} for Cr^{3+} [2], −5.4 cm^3mol^{-1} for Fe^{3+} [3].

The aim of this work is to obtain the volume of activation for a trivalent aqua ion known unambiguously to undergo dissociative activation for substitution. Al(III) was chosen because it reacts *via* a dissociative (*D*) mechanism in non-aqueous solvents, as shown by the large positive activation volumes [4], and also because it is accepted [5] that complex formation reactions in aqueous solution involving this cation follow the *Eigen-Wilkins* mechanism, with loss of a H_2O molecule as the rate-determining step.

Two variable-temperature studies of H_2O exchange on $Al(H_2O)_6^{3+}$ have already been performed, with discordant results. One of the problems encountered in these studies is the overlap of the bulk-H_2O signal and the kinetically interesting coordinated-H_2O signal. To separate the two signals *Fiat* and *Connick* [6] added the paramagnetic shift reagent Co(II) which causes a large average chemical shift of the bulk-H_2O resonance due to the strong interaction between the rapidly exchanging bulk H_2O and the paramagnetic ions. More recently, *Neely* [7], to extend the accessible temperature range, added the rapidly

[1] Part 25 of the series 'High-Pressure NMR Kinetics'. Part 24: [1].

[2] These results are part of the Ph. D. thesis of *D. H.-C.*, University of Lausanne, 1984.

exchanging Mn(II) as paramagnetic relaxation reagent, which causes the bulk-H_2O signal to disappear into the base-line.

Another problem is the facile hydrolysis of Al(III) in H_2O. This can easily be overcome by the addition of a strong acid. It has been shown [8] by ^1H- and ^{27}Al-NMR that in acidified solutions with a poorly coordinating counter-ion, even with a high Al^{3+} content, only the monomeric species $Al(H_2O)_6^{3+}$ is present.

In this study of H_2O exchange on $Al(H_2O)_6^{3+}$ as a function of temperature and pressure, we have used Mn(II) as a relaxation agent and have acidified the samples with $HClO_4$. To extend even further the accessible temperature range for a more accurate determination of the kinetic parameters we have used fast-injection ^{17}O-NMR.

Experimental. – 1. *Chemicals and Solutions.* All samples were prepared using commercial, analytical-grade reagents. The metal-ion content of hydrated $Al(ClO_4)_3$ and $Mn(ClO_4)_2$ was determined by complexometric titration with Na_2H_2 (EDTA) [9]. The composition of the different solns. used for the variable-temperature and variable-pressure bound-H_2O transverse relaxation-rate measurements are given in *Table 1*. They were prepared by mixing weighed quantities of $Al(ClO_4)_3 \cdot 6H_2O$ *(Fluka, purum)* and $Mn(ClO_4)_2 \cdot 6H_2O$ *(Merck, p.a.)* with the required amounts of $HClO_4$ (70%, *Merck, p.a.*) and ^{17}O-enriched H_2O (*Yeda*, Israel, *ca.* 20 or 40 atom-%, normalised in ^1H).

Table 1. *Compositions of Solutions*

Sample	1	2	3	4	5
$[Al(ClO_4)_3]$ [mol kg^{-1}]	0.50	0.50	0.49	0.50	0.50
$[Mn(ClO_4)_2]$ [mol kg^{-1}]	0.50	0.20	0.20	0.49	0.51
$[HClO_4]$ [mol kg^{-1}]	3.06	3.00	1.01	0.63	0.27
$H_2{}^{17}O$ [Atom-%]	31	32	35	17	17

The variable-temperature samples were contained in spherical glass bulbs, 8 mm o.d. with a 2 mm i.d. neck. The bulb was filled with soln., *ca.* 0.2 ml, and the neck was then heat sealed. A glass and teflon sample cell, described in [10], was used to hold the variable-pressure solns.

2. *Instrumentation.* ^{17}O-NMR spectra were recorded using a *Bruker CXP-200* spectrometer with a 4.7 T wide bore cryomagnet working at 27.11 MHz. For the variable-temp. measurements the sample temp. was held constant within ±0.3 K using a *Bruker BVT-1000* thermostating unit and was measured by a substitution technique using a Pt resistor with an accuracy of ±0.5 K at extreme temp. [11]. Variable-pressure measurements were made up to 220 MPa using the high-pressure probe described in [10]. A built-in Pt resistor is connected to an ohmmeter for temp. measurement with an accuracy of ±1.0 K after all corrections [12]. The fast-injection measurements were made using a fast-injection apparatus developed in our laboratory [13].

3. *NMR Measurements.* The variable-temperature (pressure) spectra were obtained using pulse widths of 20 μs (25 μs) in the quadrature detection mode. In both cases, we used 2 K data points resulting from 2–100 thousand scans accumulated over total spectral widths of 30–100 kHz. An exponential filter (line-proadening) of approximately 5% of the linewidth at half height of the coordinated-H_2O signal was applied to improve the signal to noise ratio. The NMR signal was fitted to a *Lorentzian* curve, and the transverse relaxation rate, $1/T_2^b$, of the H_2O coordinated to Al(III) was obtained from the linewidth at half height, $\Delta\nu_{1/2}$, corrected for the line-broadening (LB) using the relation $1/T_2^b = \pi(\Delta\nu_{1/2}\text{-LB})$. The fast injection spectra were obtained using the same conditions as for the variable-temperature measurements. However, only 1 K data points were accumulated using a rapid repetition rate of 8 ms.

Results and Data Treatment. – 1. *Variable Temperature.* If chemical exchange is slow, the ^{17}O-NMR spectrum of a dilute aqueous solution containing a hexaaqua metal ion consists of two resonances: one large, intense peak due to the bulk H_2O and a smaller peak due to the $M(H_2O)_6^{z+}$ resonance. A natural-abundance ^{17}O-spectrum of acidified $Al(ClO_4)_3$ consists of a narrow, intense signal due to the bulk H_2O at 0 ppm, and a quadruplet at +289 ppm due to ClO_4^- [14]. The bound-H_2O signal is invisible on this

spectrum. The addition of Mn(II) ion to the solution causes rapid relaxation of the bulk H_2O and the bound-H_2O peak is now apparent at +6 ppm. Mn(II) ion is a very efficient relaxation agent for the bulk-H_2O signal due to its long electron relaxation time and its very fast coordinated/bulk H_2O exchange rate. It has been shown to have no effect on the bound-H_2O linewidth [15]. The ^{27}Al spectra at various temperatures and pressures showed only one peak, due to $Al(H_2O)_6^{3+}$, thus there was no indication that hydrolysed species or inner-sphere perchlorate complexes were present.

In the slow-exchange limit, the transverse relaxation rate of Al(III)-bound H_2O is given by *Eqn. 1*, where τ is the mean life-time of H_2O in the first coordination sphere, and T_{2Q}^b is the quadrupolar relaxation time.

$$1/T_2^b = 1/\tau + 1/T_{2Q}^b \tag{1}$$

From transition-state theory, the temperature dependence of τ and its relation to k_{ex}, the pseudo-first-order rate constant for the exchange of a particular H_2O molecule [16], is described by *Eqn. 2*, where ΔS^* and ΔH^* are the entropy and enthalpy of activation, respectively, and the other symbols have their usual meanings.

$$1/\tau = k_{ex} = \frac{k_B T}{h} \cdot \exp(\Delta S^*/R - \Delta H^*/RT) \tag{2}$$

An *Arrhenius* temperature-dependence can be assumed for the quadrupolar relaxation rate *(Eqn. 3)*, where $(1/T_{2Q}^b)^{298}$ is the contribution at 298.15 K and E_Q^b is the corresponding activation energy

$$1/T_{2Q}^b = (1/T_{2Q}^b)^{298} \cdot \exp[E_Q^b/R(1/T - 1/298.15)] \tag{3}$$

Fig. 1 shows the temperature dependence of the transverse relaxation rate for 5 different samples, the compositions of which are given in *Table 1*. It is clear that, under the conditions and the concentrations used, $1/T_2^b$ is independent of the concentrations of

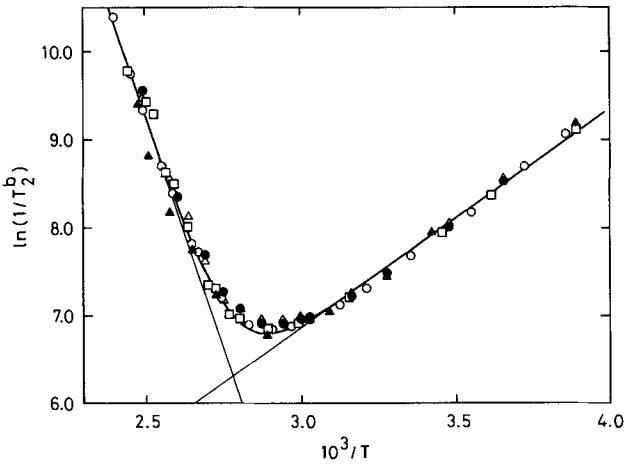

Fig. 1. *Temperature dependence of $1/T_2^b$ from the bound-H_2O ^{17}O-NMR signal of $Al(ClO_4)_3$ solutions with various concentrations of $Mn(ClO_4)_2$ and $HClO_4$.* The numbers in parentheses refer to the sample compositions given in *Table 1*. ○ (1), ● (2), △ (3), ▲ (4), □ (5). (—) $1/T_2^b$, (—) $1/\tau$ (left) and $1/T_{2Q}^b$ (right). To clarify the illustration, only half of the experimental data are shown. Every second value from each sample was chosen. All data were used in the calculation.

Table 2. *Activation Parameters and Correlation-Coefficient Matrices Obtained from Simultaneous Analyses of Variable-Temperature Data.* Data from linewidth measurements alone (A), with inclusion of low temperature k_{ex} values determined by fast injection (B).

			ΔH^*	ΔS^*	$(1/T_{2Q}^b)^{298}$	E_Q^b
A)	k_{ex}^{298} [a]) $[s^{-1}]$	1.9 ± 0.2	0.99	1.00	0.32	0.46
	ΔH^* $[kJ\ mol^{-1}]$	81.04 ± 1.03	1.00			
	ΔS^* $[JK^{-1}\ mol^{-1}]$	$+32.26 \pm 2.61$	1.00	1.00		
	$(1/T_{2Q}^b)^{298}$ $[s^{-1}]$	2276 ± 24	0.30	0.30	1.00	
	E_Q^b $[kJ\ mol^{-1}]$	21.33 ± 0.28	0.44	0.43	0.14	1.00
B)	k_{ex}^{298} [a]) $[s^{-1}]$	1.29 ± 0.04	0.90	1.00	0.10	0.17
	ΔH^* $[kJ\ mol^{-1}]$	84.74 ± 0.32	1.00			
	ΔS^* $[JK^{-1}\ mol^{-1}]$	$+41.58 \pm 0.83$	0.99	1.00		
	$(1/T_{2Q}^b)^{298}$ $[s^{-1}]$	2297 ± 24	0.04	0.05	1.00	
	E_Q^b $[kJ\ mol^{-1}]$	20.75 ± 0.27	0.05	0.08	0.08	1.00

[a]) Values obtained when the function relating k_{ex} to ΔS^* and ΔH^* was replaced by that relating k_{ex} to k_{ex}^{298} and ΔH^*. The other elements were unchanged and so are not listed.

both Mn(II), 0.2 and 0.5 *m*, and H^+, 0.27 to 3.06 *m*. Since $1/T_2^b$ is not acid-dependent, the possibility of exchange on hydrolyzed species can be ruled out. All of the data were fitted to *Eqns. 1, 2,* and *3* using a non-linear least-squares iteration programme. The exchange and NMR parameters, together with the correlation coefficient matrices are listed in *Table 2A*. Calculations using the data-set from each sample separately showed no significant difference from the parameters shown in *Table 2A*.

It is clear from *Fig. 1* that $1/T_2^b$ is dominated by the quadrupolar relaxation term over most of the temperature domain under study. Thus, k_{ex}^{298} results from the difference of two large quantities, with the large errors that ensue. The correlation-coefficient matrix in *Table 2A* shows the significant correlation between the kinetic and quadrupolar parameters. To decrease this interdependence, we performed two fast-injection experiments.

The experiments were made at 257.4 K (254.5 K). Of a thermostated solution, 1.05 *m* (0.88 *m*) in $Al(ClO_4)_3$ and 3.56 *m* (2.62 *m*) in $HClO_4$ in ordinary H_2O, 0.6 ml were injected into *ca.* the same volume of a thermostated solution, 0.83 *m* (0.82 *m*) in $Mn(ClO_4)_2$ and 3.35 *m* (2.52 *m*) in $HClO_4$ in 25 (38) atom-% $H_2{}^{17}O$, contained in a spinning 10-mm NMR tube. The final concentrations after mixing were 0.44 *m* (0.41 *m*) in $Al(ClO_4)_3$, 0.48 *m* (0.44 *m*) in $Mn(ClO_4)_2$, 3.44 *m* (2.57 *m*) in $HClO_4$, and 11 (17) atom-% in $H_2{}^{17}O$. The $Al(H_2O)_6^{3+}$ begins to exchange its H_2O with the ^{17}O-enriched H_2O, and the growth of the ^{17}O-NMR signal from the bound H_2O is measured with time. The data were fitted according to *Eqn. 4*, where $h_{b\infty}$ is the height of the bound water peak at t_∞ and P_m is the mole fraction of coordinated H_2O [17].

$$h_b = h_{b\infty}\left(1 - \exp\left(\frac{-kt}{1 - P_m}\right)\right) \tag{4}$$

One experiment at 254.5 K is illustrated in *Fig. 2*. The upper part of the figure shows some spectra while the experimental data and calculated curve are shown in the lower part. The rate constants determined at 257.4 K and 254.5 K were $(4.91 \pm 0.05) \cdot 10^{-3}\ s^{-1}$ and $(2.93 \pm 0.07) \cdot 10^{-3}\ s^{-1}$, respectively.

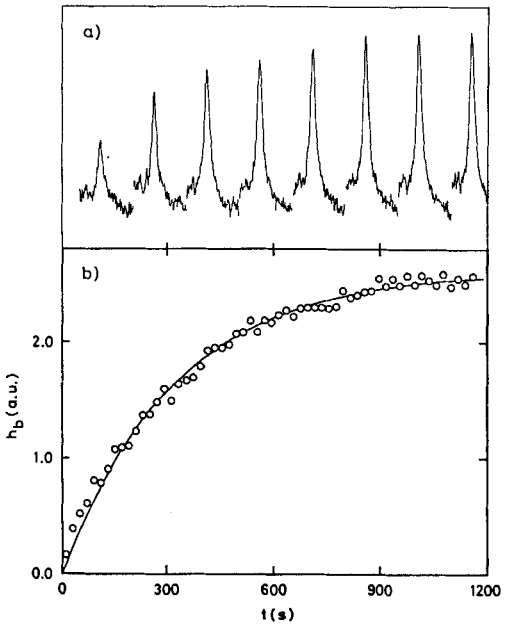

Fig. 2. *Spectra* (a) *and height* (b), *as a function of time, of the* ^{17}O*-NMR signal of coordinated* H_2O *after addition of* $Al(H_2O)_6^{3+}$ *to* ^{17}O*-enriched* H_2O. $T = 254.5$ K. Sample composition (see *Experimental*): 0.41 *m* Al^{3+}, 0.44 *m* Mn^{2+}, and 2.57 *m* H^+. Calculated $k_{ex} = (2.93 \pm 0.07) \cdot 10^{-3}\ s^{-1}$.

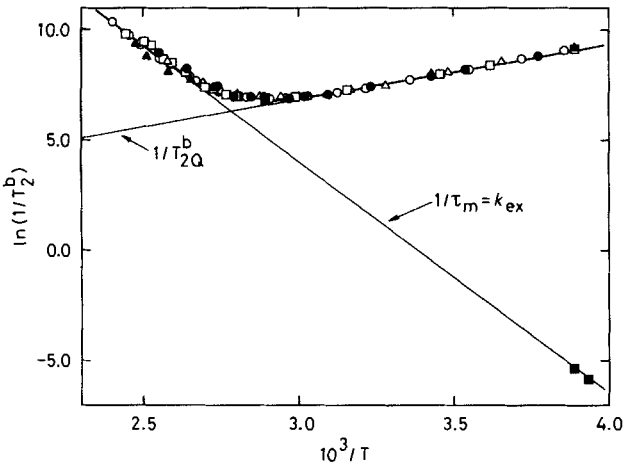

Fig. 3. *Temperature dependence of* $1/T_2^b$ *from the bound-*H_2O ^{17}O*-NMR signal of* $Al(ClO_4)_3$ *solutions with various concentrations of* $Mn(ClO_4)_2$ *and* $HClO_4$. k_{ex} (■) obtained from fast-injection experiments. Other symbols as in *Fig. 1*.

These low-temperature k_{ex} values were added to the $1/T_2^b$ data and a combined analysis of all results gave the final set of NMR and exchange parameters listed in *Table 2B* along with the correlation-coefficient matrix of the computer fit. The experimental data and calculated curve are illustrated in *Fig. 3*. We can see from the figure that the chemical exchange rate is defined over all of the temperature domain covered in our study. Consequently, the strong correlation between the kinetic and quadrupolar parameters, visible in the fit of the $1/T_2^b$ data alone, is practically eliminated. The correlation-coefficient matrix in *Table 2B* shows that the kinetic and quadrupolar contributions to $1/T_2^b$ are practically independent of one another. The exchange parameters are known to a higher

degree of accuracy, as shown by the reduced standard deviations of the exchange activation parameters *(Table 2B)*. The standard deviations of the exchange parameters resulting from the combined analysis are almost three times smaller than the standard deviations of the parameters obtained solely from $1/T_2^b$ measurements.

2. *Variable Pressure.* The variable-pressure dependence of the transverse relaxation rate can be described by two equations. *Eqn. 5* is a quadratic expression relating the pressure dependence of k_{ex}, the pseudo-first-order rate constant for exchange, ΔV_{ex}^*, the activation volume for the exchange process, $\Delta\beta^*$, the compressibility of activation, and k_0, the exchange rate at zero pressure [18].

$$\ln k_{ex} = \ln k_0 - \frac{\Delta V_{ex}^* P}{RT} + \frac{\Delta\beta^* P^2}{2RT} \tag{5}$$

The pressure dependence of the ln of the quadrupolar relaxation rate can be described by a linear equation where $(1/T_{2Q}^b)_0$ is the contribution at zero pressure and ΔV_Q^* is the quadrupolar activation volume.

$$\ln\left(\frac{1}{T_{2Q}^b}\right) = \ln\left(\frac{1}{T_{2Q}^b}\right)_0 - \frac{\Delta V_Q^* P}{RT} \tag{6}$$

We measured the transverse relaxation rate as a function of pressure up to 220 MPa for 2 different sample compositions *(Table 1)*, and at 14 temperatures between 273 and 395 K. The experimental data are illustrated in *Fig. 4*. At high temperatures $1/T_2^b$ decreases with pressure and at low temperatures $1/T_2^b$ increases with increasing pressure. We attributed these observations to the pressure dependence of k_{ex} at high temperatures, to the effect of pressure on the quadrupolar relaxation rate at low temperatures, and to a combination of

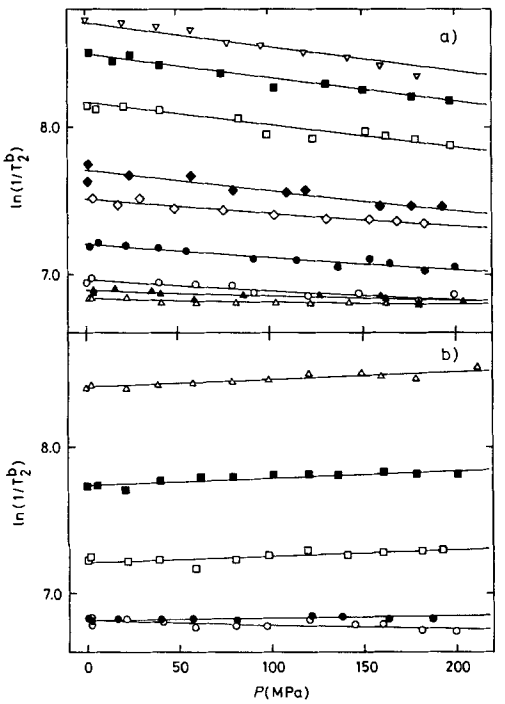

Fig. 4. *Pressure dependence of $1/T_2^b$ from the bound-H_2O ^{17}O-NMR signal of $Al(ClO_4)_3$ solutions.* The numbers in parentheses refer to the sample compositions listed in *Table 1*. a) ▽ 394.5 K (1), ■ 391.2 K (2), □ 386.9 K (1), ◆ 377.7 K (1), ◇ 371.3 K (2), ● 367.8 K (1), ○ 362.9 K (1), ▲ 355.9 K (1) ○ 350.3 K (2); b) ○ 349.6 K (1), ● 341.3 K (1), □ 313.2 K (1), ■ 292.9 K (1), △ 273.6 K (1).

these effects at intermediate temperatures. Thus, we fitted all of the data simultaneously to *Eqns. 1, 5* and *6*. In theory, k_0 and $(1/T_{2Q}^b)_0$ at each temperature could be fixed at the values obtained from the variable-temperature analysis at atmospheric pressure. In practise, small variations in concentration, field homogeneity corrections, and differences in temperature calibration between the variable-temperature and variable-pressure experiments could cause non-random errors in the $1/T_2^b$ measurements. Thus, all of the k_0 and $(1/T_{2Q}^b)_0$ values were left as adjustable parameters, except at temperatures above 377.7 K and below 341.3 K where $(1/T_{2Q}^b)_0$ and k_0, respectively, comprised less than 15% of $1/T_2^b$ and were fixed at their atmospheric-pressure values. Twenty k_0's and $(1/T_{2Q}^b)_0$'s, ΔV_{ex}^*, $\Delta\beta^*$, and ΔV_Q^* were, therefore, fitted simultaneously. Two different fits were performed. In the first instance, $\Delta\beta^*$ was assumed to be zero, *i.e.* ΔV_{ex}^* was considered to be pressure-independent. The results of this fit are given in *Table 3*. Next, $\Delta\beta^*$ was left as an adjustable parameter. The results of that fit are as follows: $\Delta V_{ex}^* = +6.6 \pm 0.7$ cm^3 mol^{-1}, $\Delta\beta^* = +(1.0 \pm 0.7) \cdot 10^{-2}$ cm^3 mol^{-1} MPa^{-1}, $\Delta V_Q^* = -1.2 \pm 0.1$ cm^3 mol^{-1}. The k_0 and $(1/T_{2Q}^b)_0$ values were the same, within experimental error as those obtained from the linear fit ($\Delta\beta^* = 0$). The weighted residual R factor, which describes the quality of the fit, was the same for both fits, and we considered the very small value of $\Delta\beta^*$ to be insignificant. Thus, ΔV^* obtained from the linear fit was taken as the definitive value.

Table 3. *Activation Parameters Derived from Measurements of $1/T_2^b$ on $Al(ClO_4)_3$ Solutions as a Function of Pressure.* Results of the linear fit for ΔV_{ex}^*.

T [K]	k_0 [s^{-1}]	$(1/T_{2Q}^b)_0$ [s^{-1}]	T [K]	k_0 [s^{-1}]	$(1/T_{2Q}^b)_0$ [s^{-1}]
394.5	5750 ± 58	297[a])	355.9	352 ± 53	635 ± 44
391.2	4582 ± 48	313	350.3	267 ± 59	663 ± 50
386.9	3199 ± 33	335	349.6	314 ± 5	595 ± 42
377.7	1832 ± 21	393	341.3	114[a])	795 ± 7
371.3	1148 ± 116	680 ± 96	313.2	7	1341 ± 12
367.8	816 ± 73	531 ± 60	292.9	1	2289 ± 20
362.9	553 ± 64	507 ± 53	273.6	0	4472 ± 41

$\Delta V_{ex}^* = +5.7 \pm 0.2$ cm^3 mol^{-1}, $\Delta V_Q^* = -1.2 \pm 0.1$ cm^3 mol^{-1}

[a]) Values without standard deviation were fixed in the data fitting procedure.

Table 4. *Kinetic Parameters for H_2O Exchange of $Al(H_2O)_6^{3+}$*

	Fiat and *Connick* [6][a])	*Neely* [7][b])	This work[b])
k_{ex}^{298} [s^{-1}]	0.2	16	1.29 ± 0.04
ΔH^* [kJ mol^{-1}]	113	65	84.7 ± 0.3
ΔS^* [JK^{-1} mol^{-1}]	+117	0	+41.6 ± 0.9
ΔV_{ex}^* [cm^3 mol^{-1}]	–	–	+ 5.7 ± 0.2

[a]) ^{17}O-NMR, using $Co(ClO_4)_2$ as a paramagnetic shift reagent.
[b]) ^{17}O-NMR, using $Mn(ClO_4)_2$ as a paramagnetic relaxation reagent.

Discussion. – The kinetic results of the present variable-temperature and variable-pressure H_2O-exchange study on $Al(H_2O)_6^{3+}$ are listed in *Table 4*, together with those from the literature. The discrepancies between the 3 sets of parameters stemming from variable-temperature measurements can easily be explained. *Fiat* and *Connick* [6] determined the kinetic line-broadening of the ^{17}O-NMR signal of the coordinated H_2O, using the Co(II) ion as paramagnetic shift reagent for the overlapping bulk-H_2O signal. Since the

Co(II) induced chemical shift is not sufficiently large at high temperatures, they only had access to part of the line-broadening chemical-exchange domain available in the present study where Mn(II) is used as relaxation reagent for the bulk H_2O. Furthermore, these authors did not have the opportunity to use a fast-injection NMR device, and consequently, their kinetically accessible temperature range was only a seventh of ours. Thus, even though their experimental data coincide with ours, their derived kinetic parameters are less accurate. *Neely* [7] also used Mn(II) to relax the free-H_2O peak and measured the bound-H_2O linewidths over a temperature range very similar to ours. However, he used non-acidified samples, and a much higher Al(III) concentration. In the kinetic exchange domain, *Neely* found higher rate constants than we did, as would be expected for exchange on hydrolysed species [2] [19]. Thus, his study cannot be interpreted simply as H_2O exchange on $Al(H_2O)_6^{3+}$. Until now, the dissociative character of H_2O exchange on $Al(H_2O)_6^{3+}$ lay only on the large, positive ΔS^* [6], and we have also found a positive ΔS^*. However, ΔS^* is not an infallible mechanistic indicator [20], and ΔV^* should provide more precise information.

First of all, let us consider the available information from non-aqueous solvent exchange on hexasolvated Al(III) in the diluent CH_3NO_2. Complete studies have been performed for the solvent dimethylsulphoxide (DMSO), dimethylformamide (DMF) and trimethylphosphate (TMPA) [4]; Activation volumes of +15.6, +13.7 and +22.5 cm^3 mol^{-1}, respectively, were determined. These large positive volumes, coupled with observed first-order-rate laws and positive ΔS^* (+22.3, +28.4 and +38.2 J K^{-1} mol^{-1}, respectively) indicate limiting dissociative (D) mechanisms. This assignment is plausible because the packing of 6 bulky solvent molecules, such as those of the solvents in question, around a small cation like Al(III) (r = 54 pm [21]) probably causes steric strain in the initial state. This strain would be relieved by the creation of a dissociative transition state, thus favouring limiting-D mechanisms. For H_2O, a relatively small molecule, we would expect the leaving group not to have completely abandoned the inner sphere of the metal ion before the entering H_2O molecule starts to coordinate. The result would be a less pronounced dissociative character. Effectively, the observed activation volume of +5.7 cm^3 mol^{-1} is well below the value of +13.5 cm^3 mol^{-1} estimated for a limiting-D, H_2O-exchange mechanism on this ion [22], although activation volumes for limiting mechanisms are difficult to estimate safely. This observed value is also less than the highest positive ΔV^* value obtained so far on hexaaquametal ion: +7.9 cm^3 mol^{-1} for the divalent Ni(II) [4]. Thus, a dissociative interchange (I_d) mechanism can reasonably be assigned to H_2O exchange on $Al(H_2O)_6^{3+}$, without totally excluding the possibility of a limiting-D mechanism.

In *Table 5*, we have listed the available data for complex formation on $Al(H_2O)_6^{3+}$ according to *Eqn. 7*. It should be noted that other simultaneous complex-formation reactions, involving the $Al(H_2O)_5(OH)^{2+}$, and protonated and unprotonated ligands as reactants, were also considered for some of the ligands studied. The corresponding other rate constants are not given, but the ligands concerned are identified by a footnote in the *Table 5*.

$$Al(H_2O)_6^{3+} + L^{n-} \underset{k_r}{\overset{k_f}{\rightleftarrows}} Al(H_2O)_5L^{(3-n)} + H_2O \qquad (7)$$

Eqn. 7 proceeds, according to the *Eigen-Wilkins* mechanism [23], in two steps: the fast formation of an outer-sphere complex, described by an equilibrium constant K_{os}, fol-

Table 5. *H_2O Exchange Rate Constant and Rate Constants for Complex Formation in Al^{3+} Aqueous Solutions at 298.2 K, according to* Eqn. 7

Ligand[a])	k_f[b]) [M^{-1} s^{-1}]	K_{os} [M^{-1}]	k_I [s^{-1}]	k_r [s^{-1}]	Method[c])	Reference
H_2O			1.29[d])			This work
$Fe(CN)_6^{3-}$	4900	7400	0.66		P-J	[26]
$Co(CN)_6^{3-}$	1600	19000	0.08		P-J	[27]
SO_4^{2-}, $I = 0.6M$[e])	15			0.74	T, P-J	[28]
SO_4^{2-}, $I = 0.0M$[e])	1200	~ 1000[f])	~ 1	0.75	T, P-J	[28]
SO_4^{2-}	775	1550[f])	0.5		P-J	[29]
$HCOO^-$	540	60	9.0		P-J	[30]
Sal^-	0.91	5.3[f])	0.17	0.78	S-F	[31]
SO_3Sal^-[e])	1.87				S-F	[32]
NO_2Sal^-[e])	0.9				S-F	[33]
Cit^-	80				S-F	[34]
SXO^{2-}[e])	24.3				Spec	[35]
$SMTB^{2-}$[e])	6.83				Spec	[35]
MTB^{2-}	0.6[g])				Spec	[36]

[a]) XSal: substituted salicylates; Cit: citrate; SXO: semixylene orange; SMT: semimethylthymol blue; MTB: methylthymol blue.
[b]) $k_f = K_{os} \cdot k_I$.
[c]) P-J: pressure-jump, T-J: temperature-jump; S-F: stopped-flow, Spec: spectrophotometry.
[d]) For the exchange of a particular H_2O molecule of $Al(H_2O)_6^{3+}$.
[e]) Reaction *via* other pathways was also considered (see text).
[f]) Calculated by the authors using the *Fuoss* equation.
[g]) k_f cannot be directly compared with any one pathway.

lowed by the rate-determining outer-sphere to inner-sphere interchange step, characterised by the rate constant k_I. These two constants are related to the experimental overall forward rate constant k_f by *Eqn. 8* if $K_{os}[L] \ll 1$.

$$k_f = K_{os} \cdot k_I \tag{8}$$

For three reactions reported in the *Table 5*, K_{os} could be obtained experimentally. In three other cases, K_{os} was estimated using the *Fuoss* equation [24] and taking into account the ionic strength with the *Davies* equation [25], leading through *Eqn. 8* to the k_I values. For the last reactions, K_{os} was neither measured nor estimated. For the substituted salicylates, the forward rate constants are comparable with that of the unsubstituted salicylate. For the other large organic ligands, k_I cannot be estimated as the application of the *Fuoss* equation to such systems is questionable [4].

For a dissociatively activated *d* substitution, k_I should be independent of the nature of the entering ligand and equal, within a statistical factor close to unity [37], to the rate constant for H_2O exchange, k_{ex}. The k_I values listed in *Table 5* are all within one order of magnitude of k_{ex}, indicating a complex-formation mechanism with rate-determining H_2O loss.

In conclusion, the positive ΔV^* clearly indicates a dissociative activation mode for H_2O exchange on Al^{3+}. This is supported by the positive ΔS^*. The similarity between k_I and k_{ex}, clearly shows that complex formation on $Al(H_2O)_6^{3+}$ is also dissociatively activated and proceeds *via* the *Eigen-Wilkins* mechanism.

We thank the *Swiss National Science Foundation* for financial support through grant 2.024-0.83.

Supplementary Material Available. – Experimental data for the variable-temperature, fast-injection and variable-pressure studies, activation parameters for each individual sample, and *Figure* of the transverse relaxation rate as a function of inverse temperature for H_2O exchange on $Al(H_2O)_6^{3+}$.

REFERENCES

[1] A. D. Hugi, L. Helm, A. E. Merbach, *Helv. Chim. Acta* **1985,** *68,* 508.
[2] Fan-Chou Xu, H.R. Krouse, T.W. Swaddle, *Inorg. Chem.* **1985,** *24,* 267.
[3] T. W. Swaddle, A. E. Merbach, *Inorg. Chem.* **1981,** *20,* 4212.
[4] A. E. Merbach, *Pure Appl. Chem.* **1982,** *54,* 1479.
[5] J. Burgess, 'Metal Ions in Solution', Ellis Horwood Ltd., Chichester, 1978.
[6] D. Fiat, R. E. Connick, *J. Am. Chem. Soc.* **1968,** *90,* 608.
[7] J. W. Neely, Ph. D. Thesis, University of California (Berkeley), 1971; Report UCRL-20580.
[8] J. W. Akitt, N. N. Greenwood, B. L. Khandelwal, G. D. Lester, *J. Chem. Soc., Dalton Trans.* **1972,** 604.
[9] E. Wänninen, A. Ringbom, *Anal. Chim. Acta* **1955,** *12,* 308.
[10] D. L. Pisaniello, L. Helm, P. Meier, A. E. Merbach, *J. Am. Chem. Soc.* **1983,** *105,* 4528.
[11] C. Ammann, P. Meier, A. E. Merbach, *J. Magn. Reson.* **1982,** *46,* 319.
[12] F. K. Meyer, A. E. Merbach, *J. Phys. E* **1979,** *12,* 185.
[13] P. Bernhard, L. Helm, A. Ludi, A. E. Merbach, *J. Am. Chem. Soc.* **1985,** *107,* 312.
[14] J. Virlet, G. Tantot, *Chem. Phys. Lett.* **1976,** *44,* 296.
[15] L. Helm, L. I. Elding, A. E. Merbach, *Helv. Chim. Acta* **1984,** *67,* 1453.
[16] T. W. Swaddle, *Adv. Inorg. Bioinorg. Mechanisms* **1983,** *2,* 95.
[17] L. I. Elding, L. Helm, A. E. Merbach. *Inorg. Chem.*, in press.
[18] H. Kelm, D. A. Palmer, 'High Pressure Chemistry', Ed. H. Kelm, D. Reidel Pub. Co., Dordrecht, 1978.
[19] M. Grant, R. B. Jordan, *Inorg. Chem.* **1981,** *20,* 3689.
[20] K. E. Newman, F. K. Meyer, A. E. Merbach, *Inorg. Chem.* **1979,** *19,* 3696.
[21] R. D. Shannon, *Acta Crystallogr., Sect. A* **1976,** *32,* 751.
[22] T. W. Swaddle, *Inorg. Chem.* **1983,** *22,* 2663.
[23] M. Eigen, R. G. Wilkins, *Adv. Chem. Ser.* **1965,** *49,* 55.
[24] R. M. Fuoss, *J. Am. Chem. Soc.* **1958,** *80,* 5059.
[25] R. A. Robinson, R. H. Stokes, 'Electrolyte Solutions', 2nd edn., Butterworths, London, 1959.
[26] M. Matüsek, H. Strehlow, *Ber. Bunsenges. Phys. Chem.* **1969,** *73,* 982.
[27] C. Kuehn, W. Knoche, *Trans. Farad. Soc.* **1971,** *67,* 2101.
[28] J. Miceli, J. Stuehr, *J. Am. Chem. Soc.* **1968,** *90,* 6967.
[29] C. Kalidas, W. Knoche, D. Papadopoulos, *Ber. Bunsenges. Phys. Chem.* **1971,** *75,* 106.
[30] H. Rauh, W. Knoche, *Ber. Bunsenges. Phys. Chem.* **1979,** *83,* 518.
[31] F. Secco, M. Venturini, *Inorg. Chem.* **1975,** *14,* 1978.
[32] B. Perlmutter-Hayman, E. Tapuhi, *Inorg. Chem.* **1977,** *16,* 2742.
[33] B. Perlmutter-Hayman, E. Tapuhi, *Inorg. Chem.* **1979,** *18,* 875.
[34] M. A. Lopez-Quintela, W. Knoche, J. Veith, *J. Chem. Soc., Faraday Trans. 1* **1984,** *80,* 2313.
[35] S. Murakami, *J. Inorg. Nucl. Chem.* **1979,** *41,* 209.
[36] T. V. Mal'kova, V. D. Ouchinnakova, *Russ. J. Inorg. Chem.* **1972,** *17,* 813.
[37] D. W. Margerum, G. R. Layley, D. C. Weatherburn, G. W. Pagenkopf, 'Coordination Chemistry', Ed. A. E. Martell, Am. Chem. Soc., Washington, 1978, Vol. 2, Chap. 1.